Korean J. Chem. Eng., 34(5), 1490-1494 (2017)
DOI: 10.1007/s11814-017-0054-9

pISSN: 0256-1115
eISSN: 1975-7220

Cu seed layer damage caused by insoluble anode in Cu electrodeposition

Yu Seok Ham*, Sung Ki Cho,†, and Jae Jeong Kim*,†**

*School of Chemical and Biological Engineering, Institute of Chemical Process, Seoul National University, Gwanak 1, Gwanak-ro, Gwanak-gu, Seoul 08826, Korea
**Department of Energy and Chemical Engineering, Kumoh National Institute of Technology, 61 Daehak-ro, Gumi-si, Gyeongsangbuk-do 39177, Korea
(*Received 1 November 2016 • accepted 27 February 2017*)

Abstract−We verified that a Cu seed layer could be damaged by a Pt insoluble anode in Cu electrodeposition. When the Cu seed layer was connected to the Pt galvanically, it was pitted and became resistive. The existence of Pt oxides on the Pt developed a potential with respect to the Cu seed layer, and accompanying electron flow from the Cu seed layer to the Pt insoluble anode. This resulted in the dissolution of the Cu seed layer, and the reduction of Pt oxides, which was confirmed by XPS analysis. The pitting current increased with the oxidation time and the surface area of the Pt, indicating the dissolution current on the Cu seed layer was associated with the Pt oxides on the Pt. This study implies that it is necessary to reduce the Pt anode regularly to prevent the Cu seed damage by the Pt anode in Cu electrodeposition.

Keywords: Cu Electrodeposition, Galvanostatic Condition, Pitting Corrosion, Cu Seed Layer Damage, Insoluble Anode

INTRODUCTION

The fabrication of Cu interconnection in electronic devices is the main application of Cu electrodeposition [1-4]. In Cu electrodeposition, the Cu seed layer is essential for providing the conductive path for the electron transfer in electrochemical reduction [5]. Also, it helps the initial nucleation of electrochemical film formation. However, the seed layer can be damaged in the electrolyte during the metallization process, resulting in increase of the resistance of Cu seed layer. Many studies have investigated the defects and the dissolution of seed layer by Cu oxide, electrolyte [6-8]. These defects can lead to physically discontinuous seed layer. Thus, voids and defects in the trench or via can be formed. In addition, oxide formation on the insoluble anode can produce the dissolution of Cu by galvanic reaction between the Cu substrate (cathode) and counter electrode (anode). The anode would be either soluble (Cu metal) or insoluble (Pt, IrOx), and the oxidation of water (to oxygen) and anode itself (to Pt oxide) occurs on the insoluble anode [9,10]. Generally, an insoluble anode is superior in the electrolyte management in the manufacturing process because the Cu anode generates passivating sludge during its dissolution [11]. In manufacturing process, the reference electrode seldom takes part in the electrodeposition system and the voltage or current between cathode and anode are being controlled (two-electrode system) by the instruments such as the plating power supply or the rectifier. In addition, the constant current (galvanostatic mode) is preferred to control the electrodeposition rate and the total deposit thickness.

In this study, we explored the possibility of seed damage induced by the use of an insoluble anode. Two-electrode systems can allow the electric connection between the substrate and anode via the circuit elements, such as the operational amplifier or the capacitors, and its deposition current is controlled by the input voltage of the instrument [12]. Within the response time (a few μs to ms depending on the instruments), it can form a galvanic cell between two electrodes. In the open circuit condition, Cu surface (Cu seed layer) is equilibrated with cupric ion in the electrolyte, whereas a Pt insoluble anode is in an equilibrium between Pt and its oxide. Accordingly, the oxidation of the Cu surface (Cu dissolution) can be induced, whereas Pt oxide is reduced to Pt in the galvanic cell. Herein, we demonstrate this seed damage induced by the insoluble Pt anode, and its change according to the various conditions on the anode.

EXPERIMENTAL

Cu-coated silicon wafers and Pt plate were used as electrodes. The silicon wafer had a multilayer structure of Cu seed layer (10, or 50 nm, PVD)/TaN (30 nm, PVD)/Ta (30 nm, PVD)/Ta (30 nm, PVD)/Si. The sheet resistance of as-prepared 10 nm Cu-coated wafer was 8.13 (±0.98) ohm/sq. The native oxide of Cu was removed via immersion into a mixture of 0.03 M citric acid and 0.034 M potassium hydroxide (2 min). The Pt plate anode was prepared via oxidation in Cu plating electrolyte (1.0 M $CuSO_4$ and 0.5 M H_2SO_4), which reproduced the equivalent condition of Pt anode used in Cu electrodeposition. It was oxidized in the Cu plating electrolyte by applying 2.0 V vs. Ag/AgCl for various time period using a potentiostat (EG&G 2273, Princeton Applied Research Corporation) (Fig. 1(a)). The oxidized Pt anode could be refreshed in 0.5 M H_2SO_4 by coulometric reduction. Fig. 1(b) is the chronopotentiogram of oxidized Pt with the various reduction current. The potential transition from positive value to negative value (hydrogen evolution) is due to the Pt oxide removal, and the short potential

†To whom correspondence should be addressed.
E-mail: jjkimm@snu.ac.kr, chosk@kumoh.ac.kr

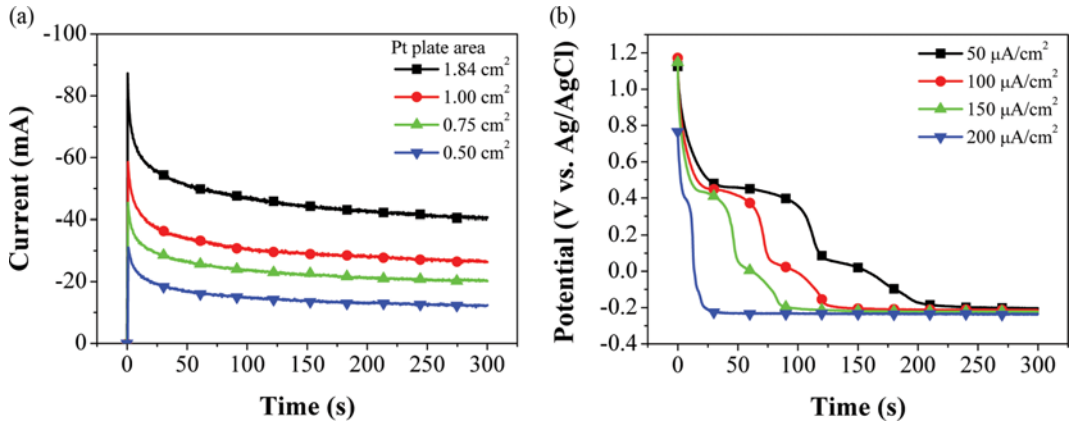

Fig. 1. (a) Chronoamperometry of Pt plate for Pt oxidation by applying 2.0 V (vs. Ag/AgCl), and (b) chronopotentiometry of oxidized Pt with various reduction current density.

plateau indicates of various oxidation state of Pt oxides [13]. After every experiment, Pt anode was refreshed by applying 100 μA/cm^2 for 3 min. The implementation of Cu seed damage was carried out in the plating electrolyte, which was purged with N_2 for 60 min beforehand and its temperature was maintained at 30 °C by using a thermostat. The Cu-coated silicon wafer loaded on a Teflon holder (with an exposed area of 1 cm^2) connected to Pt anode (1 cm^2) were immersed in the electrolyte for 60 s. A patterned wafer (Cu seed (15 nm at side wall, and 50 nm at bottom, PVD)/TaN (30 nm, PVD)/Ta (30 nm, PVD)/Ta (30 nm, PVD)/Si, width: 150 nm, depth: 300 nm) was also used to verify the effect of seed damage on the trench fill. The damaged patterned wafer was prepared as follows. The oxidized Pt (oxidized at 2.0 V vs. Ag/AgCl for 30 min in 1.0 M $CuSO_4$ and 0.5 M H_2SO_4) was connected to the Cu patterned wafer in the Cu plating electrolyte for 60 s. Then, Cu electrodeposition was carried out in 0.25 M $CuSO_4{\cdot}5H_2O$, 1.0 M H_2SO_4, 1 mM NaCl, 50 μM bis(3-sulfopropyl) disulfide, 88 μM polyethylene glycol (Mw 3400) for 60 s under applying 10 mA/cm^2. A Cu rod and Ag/AgCl saturated by KCl were used as the counter electrode and reference electrode, respectively.

The voltage and galvanic current flow between Cu seed layer and oxidized Pt was measured with a multimeter (HIOKI, DT4253). The surface defects and damage on the Cu seed layer were monitored with field emission scanning electron microscopy (FESEM, S-4800, Hitachi) and a four-point probe (CMT-SR1000N, Chang Min Tech Co.). The oxidation state of Pt before and after the current flow was surveyed with X-ray photoelectron spectroscopy (XPS, Sigma Probe).

RESULTS AND DISCUSSION

During Cu electrodeposition, cupric ions are reduced on the substrate (cathode) and Pt is oxidized into $Pt(OH)_2$, PtO and PtO_2 [14], with the simultaneous water oxidation (oxygen evolution) reaction on the Pt anode. The more positive reduction potential of Pt oxides compared to that of cupric ion can generate Cu dissolution on the substrate in the galvanic cell. The generation of defects on the Cu seed layer was monitored with varying the degree of Pt oxidation (Fig. 2). Not much change was observed on the Cu seed

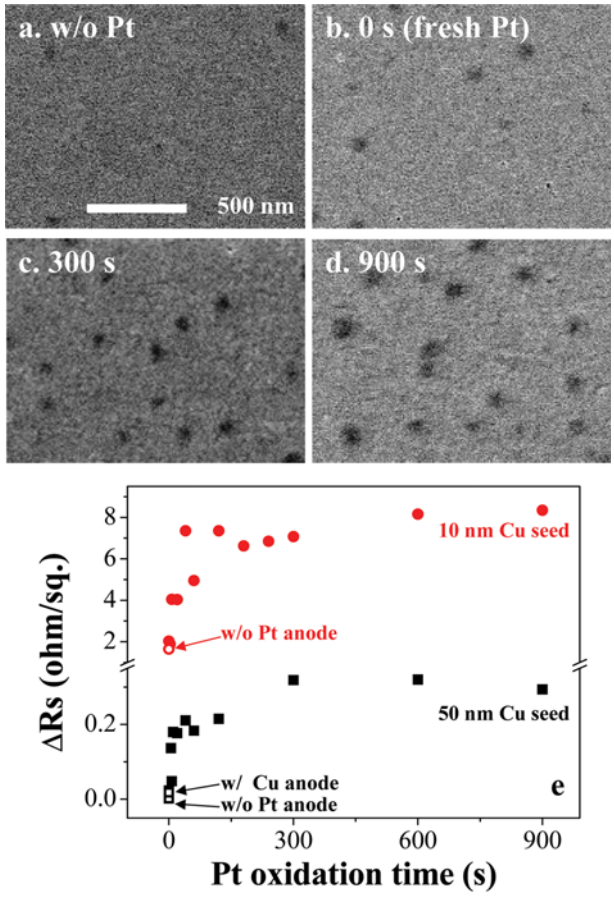

Fig. 2. (a)-(d) FESEM surface images and (e) the sheet resistance change of 50 nm Cu seed layer immersed in the plating electrolyte. Cu seed layer in the plating electrolyte was connected to Pt anode which was oxidized for various time periods beforehand.

exposed to the acidic electrolyte (Fig. 2(a)), indicating that the Cu seed layer did not have native oxide [6]. Meanwhile, many pits were clearly observed on the seed layer when it was connected to the oxidized Pt electrode (Fig. 2(b) to (d)). The sheet resistance mea-

surement could clearly show the correlation between Pt oxidation time and the extent of the damage, in terms of the overall coverage and continuity of Cu seed layer (Fig. 2(e)). Whereas, Cu seed layers connected to Cu anode or fresh Pt anode showed the negligible increase in the sheet resistance, the longer oxidation of Pt anode caused the more severe damage of the seed layer. The thinner seed layer presented more significant change in the sheet resistance, and the change was initially rapid, but it became sluggish for longer oxidation time. It is noticeable that an appreciable number of pits were generated with fresh Pt (Fig. 2(b)), though its impact on the sheet resistance was relatively small. This will be addressed later. The seed layer damage caused by oxidized Pt anode would be transferred to following Cu electrodeposition step [6], and actual defects were also found in this study after Cu electrodeposition on damaged seed layer (Fig. 3).

The potential difference and current flow between the Cu seeded substrate and the oxidized Pt anode was monitored. Contrary to the fresh Pt anode, the oxidized Pt anode built a large voltage (about 0.95 V) that was close to the theoretical value (0.84 V=1.18 V ($E^0_{Pt/Pt2+}$)–0.34 V ($E^0_{Cu/Cu2+}$)) (Fig. 4(a), (b)). The small difference might be due to the existence of a small amount of higher-order Pt oxides (PtO_3) or an activity of Cu^{2+} ([Cu^{2+}]=1 M) lower than 1. The potential difference generated current flow between the two electrodes as shown in Fig. 4(c). The sign of the current indicated electron flew from the Cu seed layer to the Pt anode; its magnitude gradually increased with Pt oxidation time, as expected. Contrary to Pt anode, Cu soluble anode did not produce a current flow, verifying that the Cu seed damage was caused by Pt anode. These are consistent with the results of the sheet resistance measurement. The current flow with fresh Pt established a background level which would accompany the generation of a small numbers of pits and a slight increase in the sheet resistance. The total charge increased with Pt oxidation time and its tendency was similar with the change of sheet resistance, that is, the extent of damage (Fig. 4(d)).

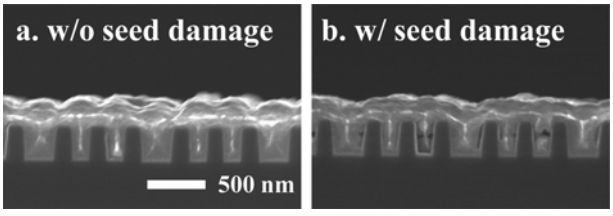

Fig. 3. Cross-sectional FESEM images of Cu electrodeposited on patterned wafer (a) without seed damage, and (b) with seed damage.

Fig. 5 shows the current flow between Cu seed layer and Pt anode with varying the surface area of Pt anode oxidized for 5 min. Obviously, the pitting current increased with the Pt surface area (Fig. 5(a)), and the total pitting charge and the change in the sheet resistance of Cu seed layer was almost linearly correlated to the change in the surface area (Fig. 5(b)). This also indicates that the damage was caused by the surface oxide of Pt anode.

XPS analysis confirmed the reduction of the Pt after current flow between the two electrodes (Fig. 6). XPS spectra from the oxidized Pt shows the existence of $Pt(OH)_2$ ($4f_{7/2}$=72.2 eV), PtO_2 ($4f_{7/2}$=75.0 eV), and Pt ($4f_{7/2}$=71.2 eV) (Fig. 6(a)). After current flow for

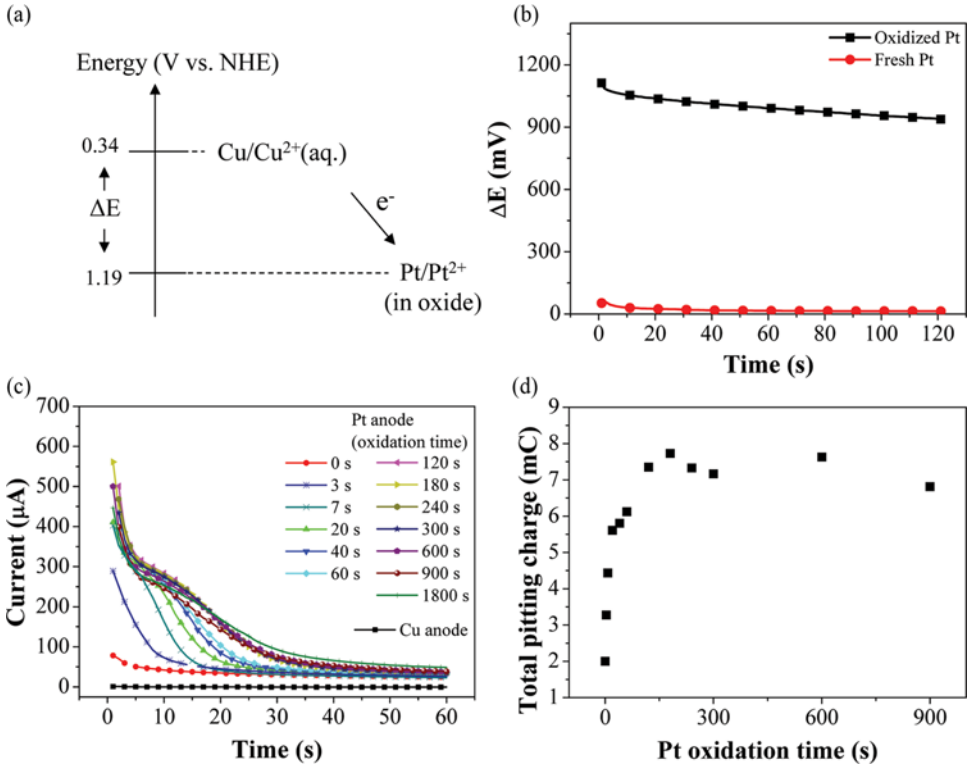

Fig. 4. (a) Energy diagram of the Cu seed layer and the oxidized Pt anode in the plating electrolyte, and (b) the potential difference and (c) current flow between the Cu seed layer and the Pt anode, and (d) the total pitting charge during the current flow.

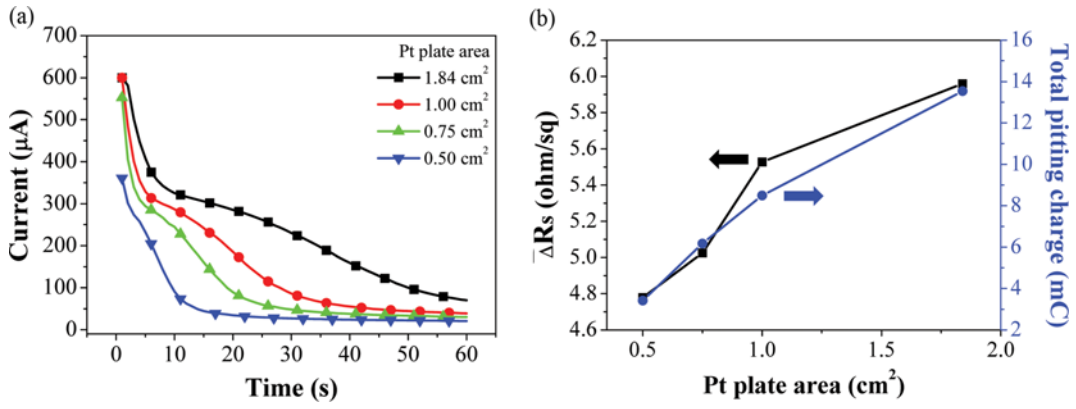

Fig. 5. (a) Current flow between the Cu seed layer and the Pt with various surface area of Pt anode, and (b) the plot of the sheet resistance change and the total pitting charge against the surface area of Pt anode.

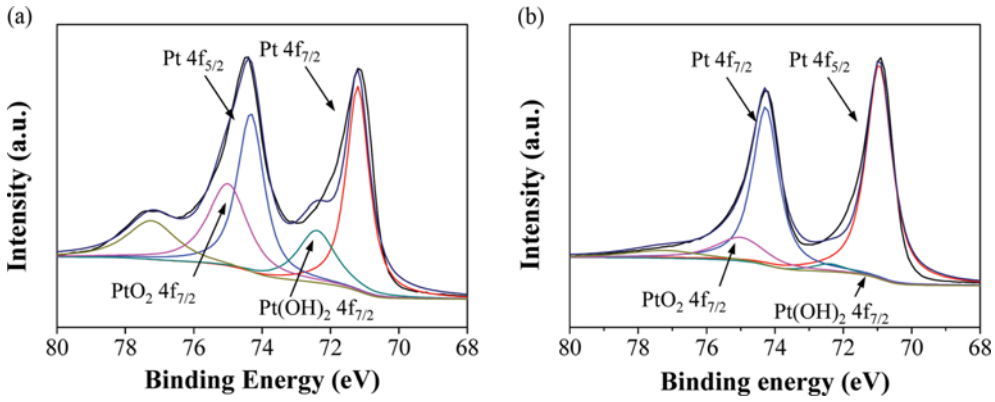

Fig. 6. XPS spectra of Pt 4f of oxidized Pt anode (a) before and (b) after connecting to Cu seed layer.

60 s, the peaks from Pt oxides decreased (Fig. 6(b)), which indicates the reduction of Pt oxide to Pt^0 on the anode and provides evidence for our speculation. Although Pt is one of the most suitable anode materials in electrochemical cells [15], it is not frequently used in industrial processes due to high cost. Instead, RuO_2 or IrO_2 coated on a titanium substrate, called dimensionally stable anodes, are more widely used in electrolyte industry [16-18]. Nevertheless, analogous phenomena are expected as Ru ($RuO_2+4H^++2e^-=Ru+2H_2O$, $E^0=0.79$ V vs. NHE) and Ir ($IrO_2+4H^++2e^-=Ir+2H_2O$, $E^0=0.93$ V vs. NHE) have high standard reduction potentials though the damage rate would depend on the electro-kinetics of each reaction.

In all cases of seed damage, the magnitude of current and relevant total charge was small and corresponds to less than 5 nm dissolution of Cu (assuming uniform dissolution). Obviously, the generation of pit resulted from uneven distribution of anodic (dissolution) current on the Cu seed layer. Our previous studies showed that dissolution of the Cu depends on the film properties, such as grain size, crystallinity, and density [19]. Since dissolution would be localized at defective site, like grain boundary, it is expected that the Cu seed layer would be pitted rather than overall thinning. Pt oxide film does not grow electrochemically beyond a few atomic layers due to its high charge transfer ability (high catalytic ability for water oxidation) and slow diffusion of oxygen through the oxide, whereby its growth rate decays rapidly [15]. Due to the limited growth of Pt oxides on the Pt surface, the amount of dissolved Cu was relatively small and was not linearly increased with Pt oxidation time. It was, however, still enough to generate local pits as dissolution occurred nonuniformly. Moreover, it would become more serious when the surface area of anode is large compared to that of Cu substrate, which is generally preferred for reducing iR drop in electrochemical systems [11]. Since current flow until whole Pt oxides were being completely reduced, it was transient and negligible after 60 s, as shown in Fig. 4(c). As the pitting current shows a maximum at the start of the current flow, the seed damage would be significant even within the short time (response time) for being a galvanic cell.

As mentioned, the galvanic connection with fresh Pt also caused the dissolution of Cu. This is associated with dissolved oxygen, which can be easily reduced on the Pt (Fig. 7(a)). While the fresh Pt did not build the potential with respect to Cu/Cu^{2+}, air purging produced the potential difference (Fig. 7(b)). The shift of the open circuit voltage of Pt in the presence of oxygen also has been observed elsewhere [15]. The relevant current flow was detected, but it was not as big as those from Pt oxides (Fig. 7(c)). The effect of dissolved oxygen would be limited by its low solubility ($[O_2]=2.7$ mM, 25 °C, 1 atm) [20], but it is still enough to generate appreciable numbers of pits as shown in Fig. 7(d).

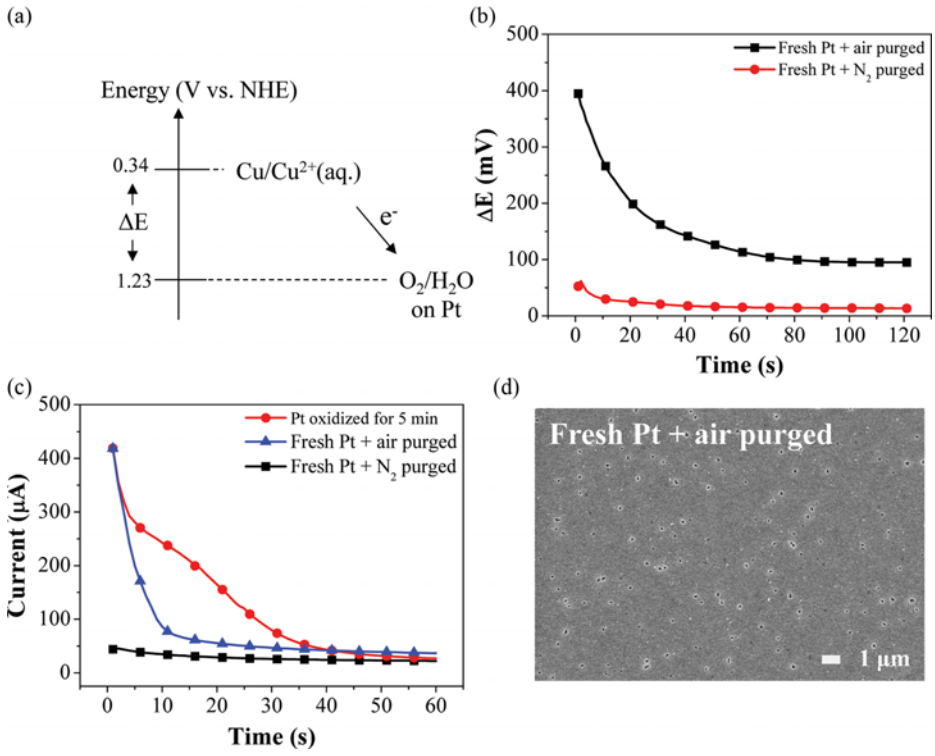

Fig. 7. (a) Energy diagram of the Cu seed layer and the Pt anode in the presence of dissolved oxygen in the plating electrolyte. (b) The potential difference and (c) current flow between the Cu seed layer and the Pt anode, and (d) FESEM surface images of the Cu seed layer after current flow.

CONCLUSIONS

The Cu seed damage induced by insoluble Pt anode was demonstrated in Cu electrodeposition. The voltage and current measurement showed that the oxide on the insoluble anode developed the potential difference between the Cu seed layer and the insoluble anode as well as corresponding current flow which was related to Cu dissolution and Pt reduction. Undesirable initial current shooting during the response time might be related to the seed damage induced by the insoluble anode. As a result, regular reconditioning via coulometric reduction, of the insoluble anode suggested in this study, could minimize this seed damage and void-free filling could be achieved.

ACKNOWLEDGEMENTS

This work was supported by the "R&D Center for reduction of Non-CO2 Greenhouse gases (2013001690004)" funded by Korea Ministry of Environment (MOE) as "Global Top Environment R&D Program", and also by the "Technology Innovation Program (10043789)" funded by the Ministry of Knowledge Economy (MKE, Korea).

REFERENCES

1. O. J. Kwon, S. K. Cho and J. J. Kim, *Korean Chem. Eng. Res.*, **47**, 141 (2009).
2. M. J. Kim and J. J. Kim, *Korean Chem. Eng. Res.*, **52**, 26 (2014).
3. N. Kulyk, C. Y. An, J. H. Oh, S. M. Cho, C. Ryu, Y. K. Ko and C.-H. Chung, *Korean J. Chem. Eng.*, **27**, 310 (2010).
4. J.-S. Kim and J.-H. Choi, *Korean J. Chem. Eng.*, **27**, 1213 (2010).
5. J. J. Kim and M. S. Kang, *Korean Chem. Eng. Res.*, **39**, 721 (2001).
6. S. K. Cho, T. Lim, H. K. Lee and J. J. Kim, *J. Electrochem. Soc.*, **157**, D187 (2010).
7. N. M. Martyak and P. Ricou, *Mater. Sci. Semicond. Process.*, **6**, 225 (2003).
8. N. M. Martyak and P. Ricou, *Mater. Chem. Phys.*, **84**, 87 (2004).
9. A.-R. Park, Y.-W. Lee, D.-H. Kwak and K.-W. Park, *Korean J. Chem. Eng.*, **32**, 1075 (2015).
10. J. Kim, S. Y. Oh, J. Y. Park and Y. Kim, *Korean J. Chem. Eng.*, **33**, 344 (2016).
11. J. W. Dini and D. D. Snyder, in Modern Electroplating, S. Mordechay, P. Milan (Eds.), Wiley (2011).
12. A. J. Bard and L. R. Faulkner, Electrochemical methods: fundamentals and applications, Wiley (1980).
13. J. J. Kim and S.-K. Kim, *Appl. Surf. Sci.*, **183**, 311 (2001).
14. F. C. Anson and J. J. Lingane, *J. Am. Chem. Soc.*, **79**, 4901 (1957).
15. H. A. Laitinen and C. Enke, *J. Electrochem. Soc.*, **107**, 773 (1960).
16. P. Duby, *Jom-J Min Met Mat S*, **45**, 41 (1993).
17. S. Trasatti, *Electrochim. Acta*, **45**, 2377 (2000).
18. S. Shin, Y.-W. Choi and J. Choi, *Mater. Lett.*, **105**, 117 (2013).
19. S. K. Cho, M. J. Kim, T. Lim, O. J. Kwon and J. J. Kim, *J. Vac. Sci. Technol. B*, **29**, 011004 (2011).
20. R. Battino, T. R. Rettich and T. Tominaga, *J. Phys. Chem. Ref. Data*, **12**, 163 (1983).